Variant surface glycoprotein expression in human African trypanosomiasis patients

Jaime So[1**], Sarah Sudlow[1**], Abeer Sayeed[1], Tanner Grudda[1], Stijn Deborggraeve[2], Dieudonné Mumba Ngoyi[3], Didier Kashiama Desamber[4], Bill Wickstead[5], Veerle Lejon[6], and Monica R. Mugnier[1*]

[1]Department of Molecular Microbiology and Immunology, Johns Hopkins Bloomberg School of Public Health, Baltimore, Maryland, United States of America

[2]Department of Biomedical Sciences, Institute of Tropical Medicine, Antwerp, Belgium[#]

[3]Department of Parasitology, Institut National de Recherche Biomédicale, Kinshasa, Democratic Republic of the Congo

[4]Programme Nationale de Lutte contre la Trypanosomiase Humaine Africaine, (PNLTHA), Ministry of Health, Kinshasa, Democratic Republic of the Congo

[5] School of Life Sciences, Queen's Medical Centre, University of Nottingham, Nottingham, NG7 2UH, United Kingdom

[6] UMR-177 Intertryp, Institut de Recherche pour le Développement, Centre de Coopération Internationale en Recherche Agronomique pour le Développement, University of Montpellier, Montpellier, France

**These authors contributed equally to the work
Current address: Médecins Sans Frontières - Access Campaign, Geneva, Switzerland

* Corresponding author
E-mail: mmugnie1@jhu.edu (MM)

Abstract

Trypanosoma brucei gambiense, an extracellular protozoan parasite, is the primary causative agent of human African Trypanosomiasis. *T. b. gambiense* is endemic to West and Central Africa where it is transmitted by the bite of infected tsetse flies. In the bloodstream of an infected host, the parasite evades antibody recognition by altering the Variant Surface Glycoprotein (VSG) that forms a dense coat on its cell surface through a process known as antigenic variation. Each VSG has a variable N-terminal domain that is exposed to the host and a less variable C-terminal domain that is at least partially hidden from host antibodies. Our lab developed VSG-seq, a targeted RNA-seq method, to study *VSG* expression in *T. brucei*. Studies using VSG-seq to characterize antigenic variation in a mouse model have revealed marked diversity in *VSG* expression within parasite populations, but this finding has not yet been validated in a natural human infection. Here, we used VSG-seq to analyze *VSGs* expressed in the blood of twelve patients infected with *T. b. gambiense*. The number of *VSGs* identified per patient ranged from one to fourteen and, notably, two *VSGs* were shared by more than one patient. Analysis of expressed *VSG* N-terminal domain types revealed that 82% of expressed *VSGs* encoded a type B N-terminus, a bias not seen in datasets from other *T. brucei* subspecies. C-terminal types in *T. b. gambiense* infection were also restricted. These results demonstrate a bias either in the underlying *VSG* repertoire of *T. b. gambiense* or in the selection of *VSGs* from the repertoire during infection. This work demonstrates the feasibility of using VSG-seq to study antigenic variation in human infections and highlights the importance of understanding *VSG* repertoires in the field.

Author Summary

Human African Trypanosomiasis is a neglected tropical disease largely caused by the extracellular parasite known as *Trypanosoma brucei gambiense*. To avoid elimination by the host, these parasites repeatedly replace their dense surface coat of Variant Surface Glycoprotein (VSG). Despite the important role of VSGs in prolonging infection, *VSG* expression during natural human infections is poorly understood. A better understanding of natural *VSG* expression dynamics can clarify the mechanisms which *T. brucei* uses to alter its VSG coat and improve how trypanosomiasis is diagnosed in humans. We analyzed the expressed *VSGs* detected in the blood of patients with trypanosomiasis. Our findings indicate that a diverse range of *VSGs* are expressed in both natural and experimental infections.

Introduction

Human African Trypanosomiasis (HAT) is caused by the protozoan parasite *Trypanosoma brucei*. *T. brucei* and its vector, the tsetse fly, are endemic to sub-Saharan Africa [1]. There are two human-infective *T. brucei* subspecies: *T. b. gambiense* which causes chronic infection in West and Central Africa (~98% of cases) and *T. b. rhodesiense* which causes acute infection in East and Southern Africa (~2% of cases) [2,3]. In humans, infections progress from an early stage that is generally marked by a fever and body aches to a late stage that begins once the parasite crosses the blood-brain barrier and is accompanied by the development of severe neurological symptoms [4]. HAT is considered fatal without timely diagnosis and treatment. While around 50 million people are at risk of infection [5], the number of annual human infections has declined significantly in recent years, with only 864 cases reported in 2019 [6]. The World Health Organization is working towards zero human transmissions of HAT caused by *T. b. gambiense* (gHAT) by 2030 [7]. Current public health initiatives to control the disease depend on case detection and treatment, complemented with vector control.

Prospects for developing a vaccine are severely confounded by the ability of African trypanosomes to alter their surface antigens [8]. As *T. brucei* persists extracellularly in the blood, lymph, and tissue fluids of the host, it is constantly exposed to host antibodies[9–12]. To evade immune recognition, the parasite periodically changes its dense Variant Surface Glycoprotein (VSG) coat. This process, referred to as antigenic variation, relies on a vast collection of thousands of VSG-encoding genes[13–16]. *T. brucei* also continually expands the number of usable antigens by constructing mosaic *VSGs*—the result of one or more recombination events between individual *VSG* genes [17,18]

The VSG contains two domains: a variable N-terminal domain of ~350-400 amino acids and a less variable C-terminal domain of ~40-80 amino acids, characterized by one or two conserved groups of four disulfide-bonded cysteines [13,19]. On the surface of trypanosomes, the VSG N-terminal domain is readily exposed to the host, while the C-terminal domain is proximal to the plasma membrane and largely hidden from host antibodies [20–22]. The N-terminal domain has been classified into two types, A and B, each of which is classified into subtypes (A1-3 and B1-2). The C-terminal domain has been classified into six types (1-6) [13,19]. These classifications are based on protein sequence patterns anchored by the conservation of cysteine residues. The biological implications of these VSG domain types have not been investigated.

Little is known about how the large genomic repertoire of *VSGs* is used in natural infections; the number and diversity of *VSGs* expressed by wild parasite populations remains unknown. One VSG in particular, LiTat 1.3, has been identified as an antigen against which a large percentage of gHAT patients have antibodies [23]. As a result, LiTat 1.3 is the main target antigen in the primary serological screening tool used for gHAT, a test known as the card agglutination test for trypanosomiasis (CATT/*T.b. gambiense*)[24]. Despite the widespread use of the CATT to screen for gHAT there are

121 shortcomings: not only can the CATT provide false negatives, but there are also *T. b.*
122 *gambiense* strains that lack the LiTat 1.3 gene entirely [25,26]. More recently developed
123 rapid diagnostic tests use a combination of native LiTat1.3 and another VSG, LiTat1.5
124 [27,28], or a combination of a VSG with the invariant surface glycoprotein ISG 65 [29].
125 Currently there is no serological test for diagnosis of *T. b. rhodesiense.*
126
127 Given the role of VSGs during infection and their importance in gHAT screening tests,
128 an improved knowledge of *VSG* expression dynamics could inform the development of
129 improved screening tests while enhancing our understanding of the molecular
130 mechanisms of antigenic variation. We developed VSG-seq, a targeted RNA-
131 sequencing method that identifies the *VSGs* expressed in any population of *T. brucei*
132 and measures the prevalence of each VSG in the population [30]. In a proof-of-principle
133 study, we used VSG-seq to gain insight into the number and diversity of *VSGs*
134 expressed during experimental mouse infections [30]. This study revealed significant
135 *VSG* diversity within parasite populations, yet found many of the same *VSGs* were
136 expressed in different infections, supporting previous reports of a “semi-predictable”
137 order to *VSG* switching [17,31,32]. Recently, similar high-throughput sequencing
138 methods have been used to characterize antigenic variation in experimental infections
139 of natural hosts for two related African trypanosome species, *T. vivax* and *T.*
140 *congolense* [33–35], suggesting that the mechanism for antigen production in some
141 animal parasites is different from models.
142
143 Whether or not findings from experimental studies of antigenic variation translate to
144 natural *T. brucei* infections is currently unknown. To our knowledge, only one study has
145 investigated *VSG* expression in wild *T. brucei* isolates [36]. For technical reasons, this
146 study relied on RNA isolated from parasites that were passaged through small animals
147 after collection from the natural host. As *VSG* expression may change during passage,
148 the data obtained from these samples is somewhat difficult to interpret. To gain a better
149 understanding of the characteristics of antigenic variation in natural *T. brucei* infections,
150 we sought to analyze *VSG* expression in *T. brucei* field isolates from which RNA was
151 directly extracted.
152
153 In this study, we used VSG-seq to determine the number and diversity of *VSGs*
154 expressed by *T. b. gambiense* in the blood of twelve patients with a *T. b. gambiense*
155 infection. To complement these data, we also analyzed published datasets from both
156 experimental mouse infections and *T. b. rhodesiense* patients. Our analysis revealed
157 that there is diverse expression of *VSGs* in *T. brucei* infection and distinct biases in
158 *VSG* expression during infection that may be unique to the *T. b. gambiense* subspecies.

Methods

Ethics statement

The blood specimens from *T.b. gambiense* infected patients were collected within the projects "Longitudinal follow-up of CATT seropositive, trypanosome negative individuals (SeroSui) and "An integrated approach for identification of genetic determinants for susceptibility for trypanosomiasis (TrypanoGEN) [37]. In France, the SeroSui study received approval from the "Comité Consultatif de Déontologie et d'Ethique" (CCDE) of the French National Institute for Sustainable Development Research (IRD, May 2013 session), and in Belgium from the Institutional Review Board of the Institute of Tropical Medicine (reference 886/13) and from the Ethics Committee of the University of Antwerp (B300201318039). In DR Congo, the projects SeroSui and TrypanoGEN were approved by the Ministry of Health through the Ngaliema Clinic of Kinshasa (references 422/2013 and 424/2013). Participants gave their written informed consent to participate in the projects. For minors, additional written consent was obtained from their legal representative.

Patient Enrollment and Origin Map

Patients originated from the Democratic Republic (DR) of the Congo and were identified in the second half of 2013, either during passive screening at the center for HAT diagnosis and treatment of the hospital of Masi Manimba, or during active screening by the mobile team of the national sleeping sickness control program (PNLTHA) in Masi Manimba and Mosango health zones (Kwilu province, DR Congo). Individuals were screened for the presence of specific antibodies in whole blood with the CATT test. For those reacting blood positive in CATT, twofold serial plasma dilutions of 1/2-1/32 were also tested and the CATT end titer was determined. CATT positives underwent parasitological confirmation by direct microscopic examination of lymph (if enlarged lymph nodes were present), and examination of blood by the mini-anion exchange centrifugation technique on buffy coat [38]. Individuals in whom trypanosomes were observed underwent lumbar puncture. The cerebrospinal fluid was examined for white blood cell count and presence of trypanosomes to determine the disease stage and select the appropriate treatment. The patients were questioned about their place of residence, the geographic coordinates of the corresponding villages were obtained from the atlas of HAT [39] and plotted on a map of the DR Congo using ArcGIS® software by Esri. Distances were determined and a distance matrix generated (see Supplemental Table 2).

Patient Blood Sample Collection and Total RNA Isolation

A 2.5 mL volume of blood was collected from each patient in a PAXgene Blood RNA Tube. The blood was mixed with the buffer in the tube, aliquoted in 2 mL volumes and frozen in liquid nitrogen for a maximum of two weeks. After arrival in Kinshasha, tubes were stored at -70°C. Total RNA was extracted and isolated from each blood sample as previously described [40].

205 **Estimation of Parasitemia**
206 Two approaches were used to estimate parasitemia. First, a 9 mL volume of blood on
207 heparin was centrifuged, 500 microliters of the buffy coat were taken up and
208 trypanosomes were isolated using the mini-anion exchange centrifugation technique.
209 After centrifugation of the column eluate, the number of parasites visible in the tip of the
210 collection tube were estimated. Second, Spliced Leader (SL) RNA expression levels
211 were measured by real-time PCR as previously described [40]. A Ct value was
212 determined for each patient blood sample. Real-time PCR was performed on RNA
213 samples before reverse transcription to verify the absence of DNA contamination.
214
215
216 **RNA-sequencing**
217 DNase I-treated RNA samples were cleaned up with 1.8x Mag-Bind TotalPure NGS
218 Beads (Omega Bio-Tek, # M1378-01). cDNA was generated using the SuperScript III
219 First-strand synthesis system (Invitrogen, 18080051) according to manufacturer's
220 instructions. Eight microliters of each sample (between 36 and 944 ng) were used for
221 cDNA synthesis, which was performed using the oligo-dT primer provided with the kit.
222 This material was cleaned up with 1.8x Mag-Bind beads and used to generate three
223 replicate library preparations for each sample. These technical replicates were
224 generated to ensure that any *VSGs* detected were not the result of PCR artifacts[41,42].
225 Because the number of parasites in each sample was expected to be low, we used a
226 nested PCR approach for preparing these VSG-seq libraries. First, we amplified *T.*
227 *brucei* cDNA from the parasite/host cDNA pool by PCR using a spliced leader primer
228 paired with an anchored oligo-dT primer (SL-1-nested and anchored oligo-dT;
229 Supplemental Table 1). 20 cycles of PCR were completed (55ºC annealing, 45s
230 extension) using Phusion polymerase (Thermo Scientific, #F530L). PCR reactions were
231 cleaned up with 1.8x Mag-Bind beads. After amplifying *T. brucei* cDNA, a *VSG*-specific
232 PCR reaction was carried out using M13RSL and 14-mer-SP6 primers (see primers;
233 Supplemental Table 1). 30 cycles of PCR (42ºC annealing, 45s extension) were
234 performed using Phusion polymerase. Amplified *VSG* cDNA was then cleaned up with
235 1X Mag-Bind beads and quantified using a Qubit dsDNA HS Assay (Invitrogen
236 Q32854). Sequencing libraries were prepared from 1 ng of each VSG PCR product
237 using the Nextera XT DNA Library Prepa-ration Kit (Illumina, FC-131-1096); this was
238 done according to the manufacturer's protocol with the exception of the final cleanup
239 step which was performed using 1X Mag-Bind beads. Single-end 100bp sequencing
240 was performed on an Illumina HiSeq 2500. Raw data are available in the NCBI
241 Sequence Read Archive under accession number PRJNA751607.
242
243
244 **VSG-seq analysis of *T. b. gambiense* and *T. b. rhodesiense* sequencing libraries**
245 For the analysis of both *T. b. gambiense* (VSG-seq preparations) and *T. b. rhodesiense*
246 (traditional mRNA sequencing library preparations; sequences were obtained from ENA,
247 accession numbers PRJEB27207 and PRJEB18523) raw reads were processed using
248 the VSG-seq pipeline available at https://github.com/mugnierlab/VSGSeqPipeline.
249 Briefly, *VSG* transcripts were assembled *de novo* from quality- and adapter-trimmed
250 reads for each sample (patient or patient replicate) from raw reads using Trinity (version

5.26.2) [43]. Contigs containing open reading frames (ORFs) were identified as previously described [30]. ORF-containing contigs were compared to Lister427 and EATRO1125 *VSGs* as well as a collection of known contaminating non-*VSG* sequences. Alignments to *VSGs* with an E-value below $1x10^{-10}$ that did not match any known non-*VSG* contaminants were identified as *VSG* transcripts. For *T. b. gambiense* replicate libraries, *VSG* ORFs identified in any patient replicate were consolidated into a sole reference genome for each patient using CD-HIT (version 4.8.1)[44] with the following arguments: -d 0 -c 0.98 -n 8 -G 1 -g 1 -s 0.0 -aL 0.0. Final *VSG* ORF files were manually inspected. Two *T. b. gambiense* patient *VSG*s (Patients 11 and 13) showed likely assembly errors. In one case a *VSG* was duplicated and concatenated, and in another two *VSGs* were concatenated. These reference files were manually corrected (removing the duplicate or editing annotation to reflect two *VSGs* in the concatenated ORF) so that each *VSG* could be properly quantified. *VSG* reference databases for each patient are available at https://github.com/mugnierlab/Tbgambiense2021/. For *T. b. gambiense,* reads from each patient replicate were then aligned to that patient's consolidated reference genome using Bowtie with the parameters *-v 2 -m 1 -S* (version 1.2.3)[45] . For *T. b. rhodesiense,* each patient's data was aligned to its own *VSG* ORF assembly. RPKM values for *VSG* expression in each sample were generated using MULTo (version 1.0) [46], and the percentage of parasites in each population expressing a *VSG* was calculated as described previously [30]. For *T. b. gambiense* samples, we included only *VSGs* with an expression measurement above 1% in two or more patient replicates in our analysis. For *T. b. rhodesiense* samples, we included only *VSGs* with expression >0.01%. To compare *VSG* expression between patients, despite the different reference genomes used for each patient, CD-HIT was used to cluster *VSG* sequences with greater than 98% similarity among patients, using the same parameters as were used for consolidation of reference *VSG* databases before alignment. Each unique *VSG* cluster was given a numerical ID (e.g. Gambiense #) and the longest sequence within each group was chosen to represent the cluster. Clusters representing TgSGP and SRA were manually removed from the expressed *VSG* sets before analysis. R code used for analysis of resulting data and the generation of figures is available at https://github.com/mugnierlab/Tbgambiense2021/.

Analysis of VSG N-terminal Domains

Genomic *VSG* sequences

The *VSG* repertoires of *T. b. brucei* Lister427 ("Lister427_2018" assembly), *T. b. brucei* TREU927/4 and *T. b. gambiense* DAL972 were taken from TriTrypDB (v50). The *T. b. brucei* EATRO 1125 VSGnome was used for analysis of the EATRO1125 *VSG* repertoire (vsgs_tb1125_nodups_atleast250aas_pro.txt, available at https://tryps.rockefeller.edu/Sequences.html or GenBank accession KX698609.1 - KX701858.1). Likely VSG N-termini were identified as predicted proteins with significant similarity (e-value ≤ 10^{-5}) to hidden Markov models (HMMs) of aligned type A and B VSG N-termini taken from [15]. VSG sequences from other strains (except those generated by VSG-seq) were taken from the analysis in Cross, et al. [15].

297
298 N-terminal domain phylogenies
299 Phylogenies of VSG N-termini based on unaligned sequence similarities were
300 constructed using the method described in [47] and used previously to classify VSG
301 sequence [15]. N-termini were extracted as all predicted protein sequence up to the C-
302 terminal end of the bounding envelope of the match to either type-A or type-B HMM
303 (whichever was longer). A matrix of similarities between all sequences was constructed
304 from normalized transformed BLASTp scores as in Wickstead, et al. [47] and used to
305 infer a neighbor-joining tree using QuickTree v1.1 [48]. Trees were annotated and
306 visualized in R with the package APE v5.2 [49].
307
308 HMM
309 For N-terminal typing by HMM, we used a python analysis pipeline available at
310 (https://github.com/mugnierlab/find_VSG_Ndomains). The pipeline first identifies the
311 boundaries of the VSG N-terminal domain using the type A and type B HMM profiles
312 generated by Cross *et al.* which includes 735 previously-typed VSG N-terminal domain
313 sequences [15]. N-terminal domains are defined by the largest envelope domain
314 coordinate that meets e-value threshold ($1x10^{-5}$, --domE 0.00001). In cases where no
315 N-terminal domain is identified using these profiles, the pipeline executes a "rescue"
316 domain search in which the VSG is searched against a 'pan-VSG' N-terminus profile we
317 generated using 763 previously-typed VSG N-terminal domain sequences. This set of
318 VSGs includes several *T. brucei* strains and/or subspecies: Tb427 (559), TREU927
319 (138), *T. b. gambiense* DAL972 (28), EATRO795 (8), EATRO110 (5), *T. equiperdum*
320 (4), and *T. evansi* (21). The N-terminal domain type of these VSGs were previously
321 determined by Cross et. al (2014) by building neighbor-joining trees using local
322 alignment scores from all-versus-all BLASTp similarity searches [15]. Domain
323 boundaries are called using the same parameters as with the type A and B profiles.
324
325 After identifying boundaries, the pipeline extracts the sequence of the N-terminal
326 domain, and this is searched against five subtype HMM profiles. To generate N-terminal
327 domain subtype HMM profiles, five multiple sequence alignments were performed using
328 Clustal Omega [50] with the 763 previously-typed VSG N-terminal domain sequences
329 described above; each alignment included the VSG N-terminal domains of the same
330 subtype (A1, A2, A3, B1, and B2). Alignment output files in STOCKHOLM format were
331 used to generate distinct HMM profiles for type A1, A2, A3, B1, and B2 VSGs using the
332 pre-determined subtype classifications of the 763 VSGs using HMMer version 3.1b2
333 [51]. The number of sequences used to create each subtype profile ranged from 75 to
334 211. The most probable subtype is determined by the pipeline based on the highest
335 scoring sequence alignment against the subtype HMM profile database when HMMscan
336 is run under default alignment parameters. The pipeline generates a FASTA file
337 containing the amino acid sequence of each VSG N-terminus and a CSV with
338 descriptions of the N-terminal domain including its type and subtype.
339
340 Network graph
341 N-terminal network graphs were made using VSG N-terminal domains from TriTrypDB
342 Lister427_2018 and *T. b. gambiense* DAL972 (v50) VSG sets described above, and the

T. b. gambiense and *T. b. rhodesiense* VSG N-termini which met our expression thresholds. Identified N-terminal domains were then subjected to an all-versus-all BLASTp. A pairwise table was created that includes each query-subject pair, the corresponding alignment E-value, and N-terminal domain type of the query sequence if previously typed in Cross, et al. [15]. Pseudogenes and fragments were excluded from the Lister427_2018 reference prior to plotting by filtering for *VSG* genes annotated as pseudogenes and any less than 400 amino acids in length, as the remaining sequences are most likely to be full length VSG. Network graphs were generated with the igraph R package[52] using undirected and unweighted clustering of nodes after applying link cutoffs based on E-value < 10^{-2}. The leading eigenvector clustering method [53] was used to detect and assign nodes to communities based on clustering (cluster_leading_eigen() method in igraph).

Analysis of VSG C-terminal Domain Types

VSG C-termini were extracted from expressed *T. b. gambiense VSGs*, *T.b. gambiense* DAL972 (v50), and 545 previously-typed VSG C-termini from the Lister 427 strain using the C-terminal HMM profile generated by Cross et al.[15], and the same HMMscan parameters as for N-termini (E-value < $1x10^{-5}$; largest domain based on envelope coordinates). An all-vs-all BLASTp was performed on these sequences, and network graphs were generated in the same manner as the N-terminal network graphs. Links were drawn between C-termini with a BLASTp E-value $\leq 1x10^{-3}$. The leading eigenvector method for clustering [53] was used to detect and assign nodes to communities based on clustering (cluster_leading_eigen() method in igraph).

Results

Parasites in gHAT patients express diverse sets of VSGs

To investigate *VSG* expression in natural human infections, we performed VSG-seq on RNA extracted from whole blood collected from twelve human African trypanosomiasis patients from five locations in the Kwilu province of the Democratic Republic of Congo (Fig 1A). The relative parasitemia of each patient was estimated by SL-QPCR [54], and the number of parasites after mAECT on buffy coat was estimated for all patients except patient 29 (Table 1). RNA extracted from 2.5 mL of whole blood from each patient was used to prepare libraries for VSG-seq. *T. brucei* RNA was amplified from host/parasite total RNA using a primer against the *T. brucei* spliced leader sequence and an anchored oligo-dT primer. The resulting trypanosome-enriched cDNA was then used as a template to amplify *VSG* cDNA and submitted to VSG-seq sequencing and analysis. To determine whether a *VSG* was expressed within a patient, we applied the following stringent cutoffs:

1) We conservatively estimated that each 2.5 mL patient blood sample contained a minimum of 100 parasites. At this minimum parasitemia, a single parasite would represent 1% of the population (and consequently ~1% of the parasite RNA in a sample). As a result, we excluded all *VSGs* expressed by <1% of the population as estimated by VSG-seq.
2) We classified *VSGs* as expressed if they met the expression cutoff in at least two of three technical library replicates.

1112 unique *VSG* open reading frames were assembled *de novo* in the patient set and 44 met our expression criteria. Only these 44 *VSGs*, which we will refer to as "expressed *VSGs"* in these patient samples, were considered in downstream analysis except when noted otherwise. TgsGP, the VSG-like protein which partially enables resistance to human serum in *T. b. gambiense* [55], was assembled in samples from patients 2, 11, 13, and 17, and met expression threshold in patients 2, 11, and 17. The absence of this transcript in most samples is likely a result of the low amount of input material used to prepare samples. Notably, none of the expressed *VSGs* shared similarity with any *VSGs* in the *T. b. gambiense* DAL972 genome or the diagnostic VSGs LiTat 1.3, LiTat 1.5 and LiTat 1.6.

At least one *VSG* met our expression criteria in each patient, and in most cases multiple *VSGs* were detected. The highest diversity was observed in patient 2, with 14 *VSGs* expressed (Fig 1B, Supplemental Figure 1). We observed a correlation between parasitemia as estimated by QPCR Ct value and number of *VSGs* (Supplemental Figure 2), suggesting that these samples do not reflect the full diversity of each population. Nevertheless, two *VSG* were shared between patients: *VSG* 'Gambiense 195' was expressed in both patient 12 and patient 17 from Village C, and *VSG* 'Gambiense 38' was expressed in patient 12 from Village C and patient 23 from Village D which are 40 kilometers apart (Fig 1C).

Patient	Location	Est. parasites in 500µL buffy coat	mean SL-RNA Ct	Plasma CATT end dilution	WBC	Parasites in CSF	Stage
1	Village A	>50	22.155	≥32	1	-	First
2	Village A	>50	19.020	≥32	6	-	Early 2nd
3	Village A	2-5	28.780	≥32	6	-	Early 2nd
11	Village C	>50	22.030	4	9	-	Early 2nd
12	Village C	6-20	25.430	≥32	6	-	Early 2nd
13	Village C	6-20	26.635	16	12	-	Early 2nd
17	Village C	21-50	24.495	≥32	13	-	Early 2nd
19	Village C	1	28.245	8	7	-	Early 2nd
23	Village D	6-20	27.085	≥32	2	-	First
29	Village B	-	28.320	≥32	3	-	First
30	Village B	>50	22.960	≥32	694	+	Severe 2nd
33	Village E	1	32.385	≥32	2	-	First

Table 1. Patient stage and parasitemia data. For staging, the following definitions were used: First: 0-5 WBC/µl, no trypanosomes in CSF. Second: >5 WBC/µl or trypanosomes in CSF. (with early 2nd 6-20 WBC/µl and no trypanosomes in CSF; severe 2nd: >100 WBC/µl). WBC: white blood cells.

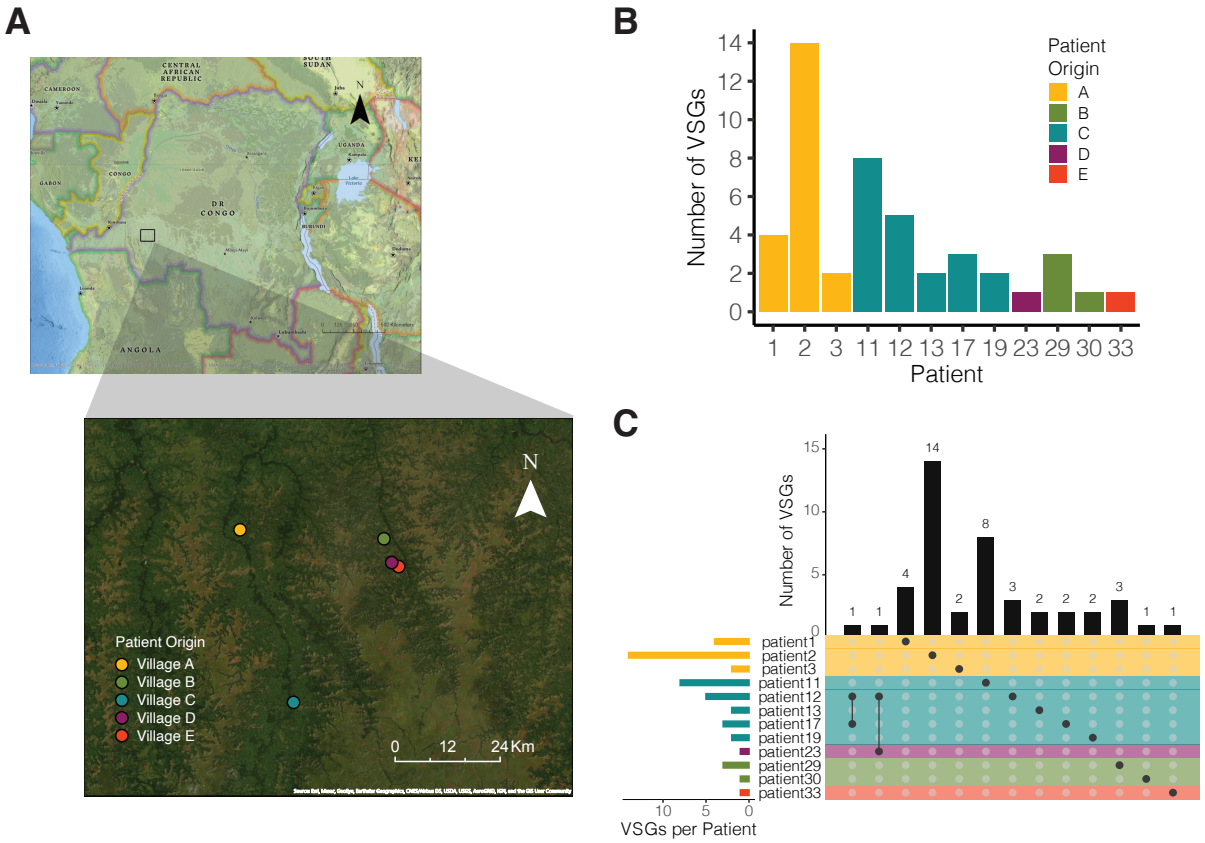

Figure 1. Parasites isolated from gHAT patients express multiple *VSGs*. (A) Map showing the location of each patient's home village. Maps were generated with ArcGIS® software by Esri, using world imagery and National Geographic style basemaps. (B) Graph depicting the

426 total number of *VSGs* expressed in each patient. (C) The intersection of expressed *VSG* sets in
427 each patient. Color indicates patient origin.

428

429 **Natural *T. b. gambiense* infections show a strong bias towards expression of type**
430 **B VSG**
431
432 To further characterize the set of expressed *VSGs* in these samples, we sought a fast
433 and unbiased method for determining the type and subtype of each VSG's N-terminal
434 domain. We evaluated two approaches. The first approach was to create a bioinformatic
435 pipeline to determine each N-terminal domain subtype that uses HMM profiles we
436 created for each subtype using sets of N-terminal domains previously typed by Cross *et*
437 *al.* [15]. The second approach was to create a BLASTp network graph based on a
438 previously published method [56] where the N-terminal subtype of a VSG is determined
439 by the set of VSGs it clusters with and clusters are identified using the leading
440 eigenvector method [53]. We used each approach to determine the N-terminal subtype
441 of each expressed *VSG* in our patient sample dataset along with 863 VSG N-termini
442 from the Lister 427 genome. We compared these results to either existing N-terminal
443 classification (for Lister 427 VSGs) or classification based on position in a newly-
444 generated BLASTp-tree[15] (for *T. b. gambiense* VSGs; Figure 2A). Both the new HMM
445 profile and BLASTp network graph approaches generally recapitulated previous VSG
446 classification based on BLASTp-tree, with all three methods agreeing 93.7% of the time
447 (Figure 2B). The HMM pipeline method agreed with BLASTp-tree typing for all patient
448 VSGs, while the network graph approach agreed for 43/44 VSGs (Figure 2B,
449 Supplemental Fig 3, Supplemental Table 1) [15]. It is not surprising that the HMM
450 pipeline would better reflect the results of the BLASTp-tree method, as the N-terminal
451 subtype HMM profiles were generated using VSGs classified by this method. Based on
452 these data, we determined the HMM method is a fast and accurate method for
453 determining the N-terminal domain types of unknown VSGs.
454
455 Our N-terminal domain typing pipeline identified the domain sequence and type for all
456 44 patient VSGs (Fig 2C). 82% of the expressed *T. b. gambiense* VSGs had type B N-
457 terminal domains, and within each patient 50% or more of expressed *VSG* were type B.
458 This bias was not restricted to highly expressed *VSGs*, as 74.5% of all assembled *VSG*
459 (813 of 1091 classifiable to an N-terminal subtype) were also type B. This observation
460 motivated further investigation into the expressed N-terminal domains in infections by
461 other *T. brucei* subspecies.
462

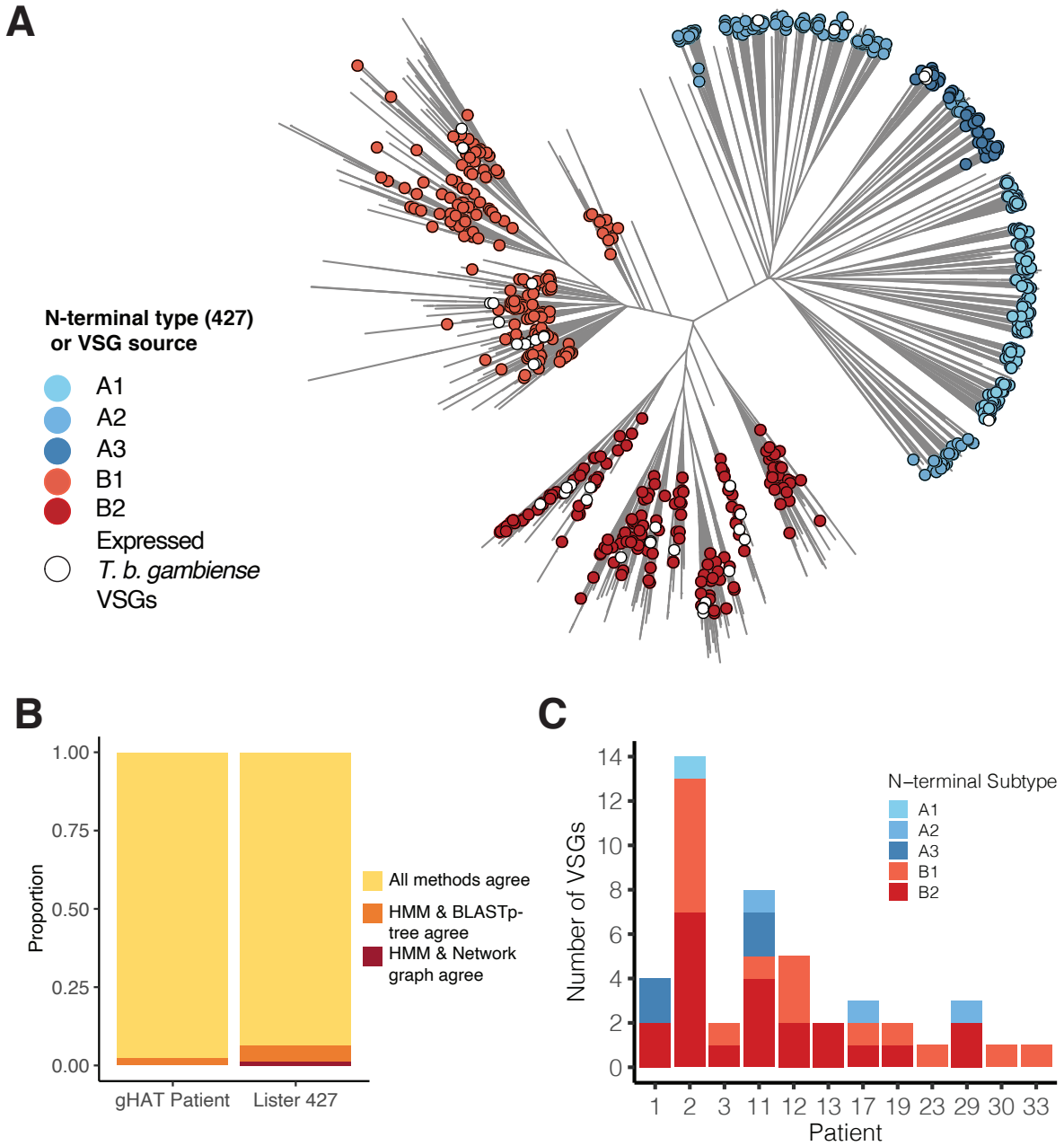

Figure 2. *T. b. gambiense* samples show a bias towards expression of type B VSG. (A) Visualization of relatedness between N-terminal domain peptide sequences inferred by Neighbor-Joining based on normalized BLASTp scores. Legend indicates classification by HMM pipeline (for Lister 427 VSGs, to highlight agreement between the two methods), or by subspecies for *VSGs* expressed in patients. (B) Agreement between three VSG typing methods for Lister 427 VSG set and the expressed *T. b. gambiense* patient VSG set. (C) N-terminal domain subtype composition of expressed *T. b. gambiense VSGs* as determined by HMM analysis pipeline.

475 **Type B VSG bias is not observed in natural *T. b. rhodesiense* infection.**
476
477 To determine whether the bias towards type B VSGs was unique to *T. b. gambiense*
478 infections, we analyzed RNA-seq data from a published study measuring gene
479 expression in the blood and cerebrospinal fluid (CSF) of *T.b. rhodesiense* patients in
480 Northern Uganda [57]. These libraries were prepared conventionally after either rRNA-
481 depletion for blood or poly-A selection for CSF samples. We analyzed only those
482 samples for which at least 10% of reads mapped to the *T. brucei* genome. Raw reads
483 from these samples were subjected to the VSG-seq analysis pipeline, and because the
484 estimated parasitemia of these patients was much higher than our *T.b. gambiense*
485 study, we adjusted our expression criteria accordingly to 0.01%, the published limit of
486 detection of VSG-seq [30]. Using this approach, we identified 77 unique *VSG*
487 sequences across all blood and CSF samples (Fig 3A, Supplemental Figure 4). SRA,
488 the VSG-like protein that confers human serum resistance in *T. b. rhodesiense* [58],
489 was expressed in all patient samples.
490
491 The HMM pipeline was able to determine types for 74 of these VSG sequences; the
492 remaining appeared to be incompletely assembled, presumably due to insufficient read
493 depth from their low level of expression. In each patient, multiple *VSGs* assembled and
494 a large proportion were expressed in multiple patients (Fig 3B), in line with our
495 observations in experimental mouse infections. Although the majority of VSGs detected
496 in these patients were type B (57%), this VSG type was much less predominant than in
497 *T. b. gambiense* infection (Fig 3C). Interestingly, there was no overlap in expressed
498 *VSGs* in the blood and CSF of patient 71, the only patient for which both blood and CSF
499 data were available for analysis, potentially indicating that different organs or body
500 compartments harbor different sets of VSGs.
501

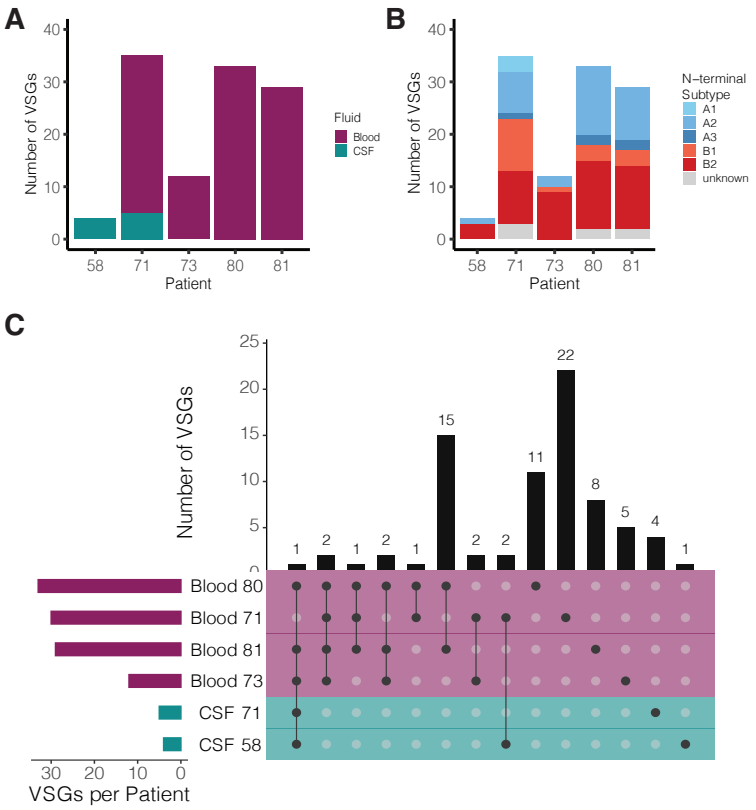

502

503 **Figure 3. *T. b. rhodesiense* samples reveal diverse *VSG* expression, but little N-terminal**
504 **type bias.** (A) The total number of expressed *T. b. rhodesiense VSG* in each patient and
505 sample type. Bar color represents sample type from which RNA was extracted. (B) N-terminal
506 domain subtype composition of all expressed *VSGs*. (C) Intersections of *VSGs* expressed in
507 multiple infections. Color represents the sample type.

508
509
510 **The predominant VSG N-terminal type fluctuates over time during experimental *T.***
511 ***b. brucei* infection**
512
513 One explanation for the bias towards type B VSG in *T. b. gambiense* could be that VSG
514 type fluctuates over time. This is plausible because patient samples only represent a
515 single moment during infection, and *T. b. gambiense* samples are more likely to be
516 obtained at a later stage of infection than *T. b. rhodesiense*. To investigate whether a
517 predominance of type B VSGs could be a feature of the chronic nature of *T. brucei*
518 *gambiense* infection, we took advantage of our published dataset derived from VSG-seq
519 analysis of parasites isolated from mice infected with the *T.b. brucei* EATRO1125 strain.
520 Blood was collected over time during this study, providing data from days 6/7, 12, 14,
521 21, 24, 26, and 30 post infection in all four mice, and from days 96, 99, 102, and 105 in
522 one of the four mice (Mouse 3). Of 192 unique VSGs identified between days 0-30 and
523 97 VSGs identified between days 96-105,190 and 93 VSGs were typed by the python
524 HMM pipeline, respectively. The remaining VSGs were incompletely assembled by
525 Trinity. Our analysis of VSG types over time revealed that the predominantly expressed

526 N-terminal domain type fluctuates between type A and type B throughout the early
527 stages of infection as well as in extended chronic infections (Fig 4). Parasitemia did not
528 correlate with either the diversity of *VSG* expression or N-terminal domain type
529 predominance (Supplemental Fig 3). Because all patient samples were collected from a
530 single timepoint, it remains unclear whether the predominant N-terminal type fluctuates
531 in human infections over time as it does in mice.
532

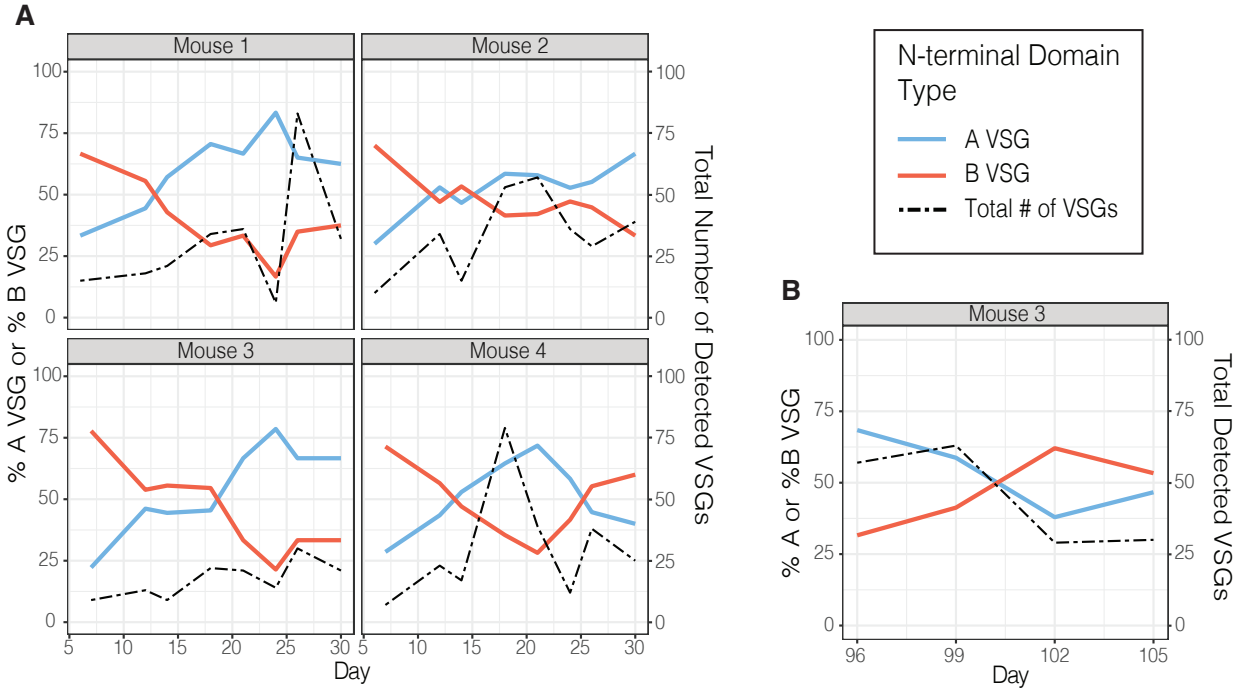

533

534 **Figure 4. VSG N-terminal type composition fluctuates over the course of infection**
535 **in mice.** Proportions of N-terminal domain types expressed in *T. b. brucei* infected mice over
536 time. Total number of identified VSGs is represented by the black dotted line. A) N-terminal type
537 composition days 0-30. B) Type composition days 96-105.

538

539 **The composition of the genomic VSG repertoire is reflected in expressed VSG N-**
540 **terminal domain types**

541

542 Another source for bias in expressed VSG type is the composition of the genomic *VSG*
543 repertoire. We were only able to make a direct comparison between the genomic and
544 expressed *VSG* repertoire for EATRO1125 mouse infections, as the 'VSGnome' for this
545 strain has been sequenced. This analysis revealed that, although the predominant N-
546 terminal VSG type fluctuates during infection, the expressed *VSG* repertoire generally
547 reflects the composition of the genomic repertoire (chi-squared p = 0.0515, Figure 5A).

548

549 Unfortunately, the full repertoire of *VSGs* encoded by most trypanosome strains is
550 unknown, so such a direct comparison is impossible for *T. b. gambiense* and *T. b.*
551 *rhodesiense* patient samples. The *T. b. gambiense* DAL972 reference genome lacks
552 most of the genomic regions containing the majority of *VSGs* (haploid arrays,

553 expression sites, and minichromosomes) and there is no publicly available *T. b.*
554 *rhodesiense* reference assembly. However, there is no significant difference in VSG
555 type frequency comparing the near-complete *T. b. brucei* Lister 427 repertoire to the
556 expressed *T. b. rhodesiense* set to which they are closely related [59] (chi-squared p-
557 value = 0.2422) (Fig 5B). Similarly, the proportion of N-terminal domains identified in
558 the *T. b. gambiense* patient samples is not statistically different from the incomplete *T.*
559 *b. gambiense* DAL972 genomic repertoire (chi-squared p-value = 0.0575) (Fig 5B). Both
560 *T. b. gambiense* patient VSG (chi-squared p-value = 2.413e-4) and the 54 VSGs
561 identified in *T. b. gambiense* DAL972 (chi-square p-value = 0.0301) have A and B type
562 frequencies that differ significantly from Lister427. Though these results should be
563 interpreted with caution given the limitations of the reference genomes being used, they
564 generally suggest that the underlying genomic *VSG* repertoire of *T. b. gambiense* differs
565 from other subspecies in its N-terminal type composition.
566

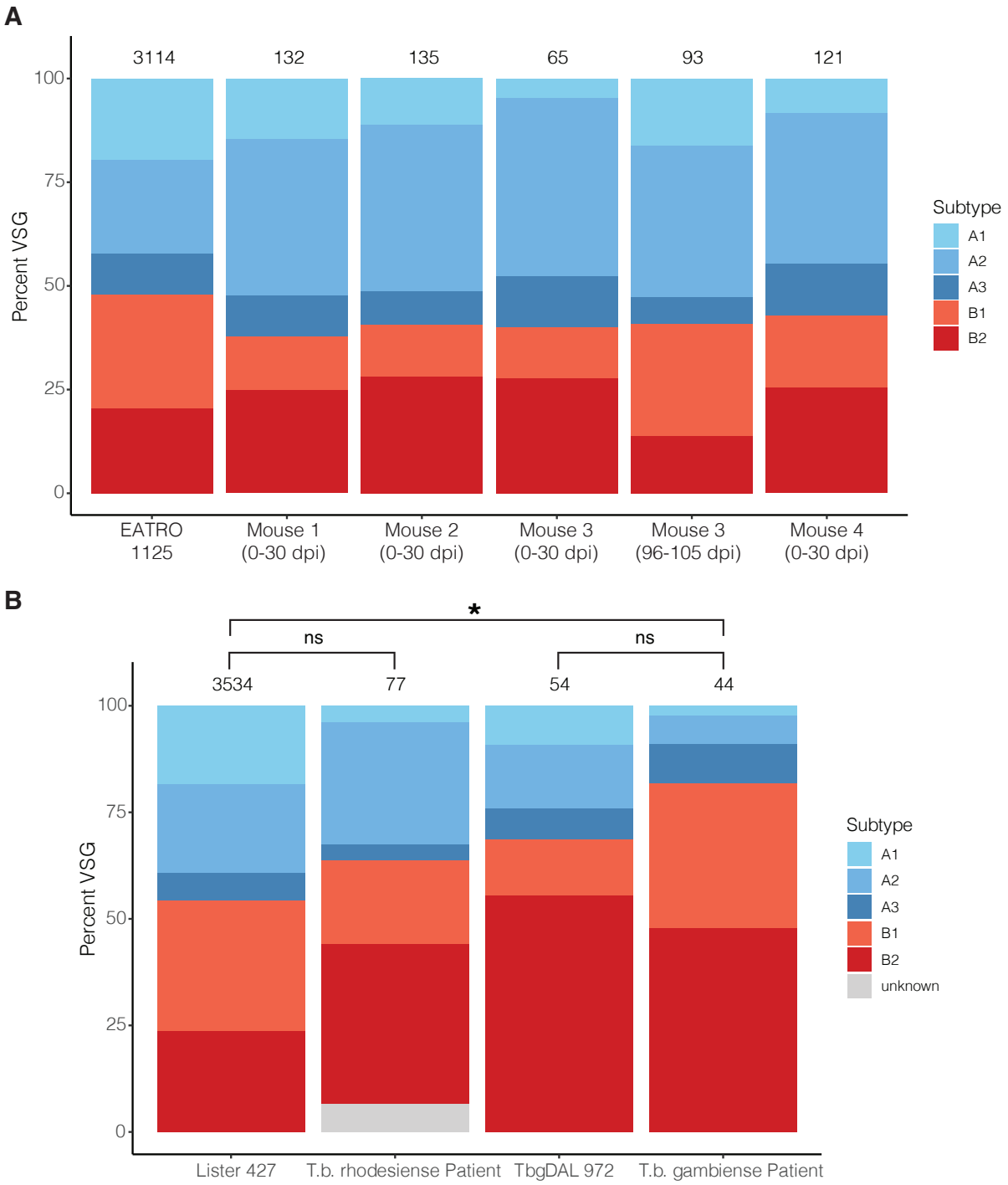

Figure 5. VSG expression reflects the genomic VSG repertoire of the infecting parasites. (A) Columns show the proportion of VSG types identified in each mouse infection over all time points. Total number of unique VSG sequences displayed above column. Mouse infections were initiated with *T.b. brucei* strain EATRO 1125. (B) A comparison of the frequencies of type A and B VSGs expressed in patients and those present in Lister 427 and DAL972 reference genomes.

573
574 ***T.b. gambiense* expressed VSG C-terminal domains show a bias for type 2**
575 **domains**
576
577 In addition to examining N-terminal types in our *T. b. gambiense* dataset, we also
578 examined expressed VSG C-termini. Previous studies defined six C-terminal types,
579 although resolution of these types in larger VSG sets has been difficult due to the high
580 level of similarity among VSG C-termini [15,56]. In line with previous observations, a
581 BLASTp-tree analysis of assembled *T.b. gambiense* C-terminal domains revealed
582 frequent sequence similarity between expressed C-terminal types but did not provide
583 sufficient resolution to confidently assign types (Fig 6A).
584
585 To supplement this analysis, we also performed a network graph analysis. Although this
586 method had previously performed poorly in resolved VSG C-termini [56], using the lead-
587 ing eigenvector clustering method [53]to define community membership within the graph
588 allowed a faithful reconstitution of the C-terminal types previously determined by
589 BLASTp tree analysis. Using this approach, we were able to tentatively assign C-termi-
590 nal domain types to the *T. b. gambiense* VSGs (Fig 6B). Most patient C-terminal domain
591 types were type 2, while the remaiing largely fell into the type 1 category. Only one type
592 3 C-terminus was identified in the patient set. Although there are very few VSG C-ter-
593 mini available in the *T. b. gambiense* DAL972 genome, these sequences show a pre-
594 dominance of types 3 and 5, while the genomic repertoire of C-termini in Lister427
595 shows roughly equivalent representation of tyeps 1, 2, and 3. Unlike *T. b. gambiense* N-
596 termini, the expressed C-termini were more restricted than the set of C-termini appar-
597 ently available in the *T. b. gambiense* DAL972 or *T. b. brucei* Lister427 genome
598 (Fisher's exact test, p-value < $1x10^{-5}$). In line with previous observations, we saw no evi-
599 dence of fomain exclusion: a C-terminal domain of one type could be paired with any
600 type of N-terminal domain (Fig 6E)[20]. As observed in our analysis of expressed N-ter-
601 mini, C-termial domain types were not correlated ot geographical origin (Fig 6F). Over-
602 all, these data suggest that, like N-termini, expressed VSG C-termini are also biased to-
603 wards certain C-terminal types. Unlike N-termini, however, C-terminal types expressed
604 in *T. b. gambiense* infection may not reflect the composition of the parasite's genomic
605 repertoire.

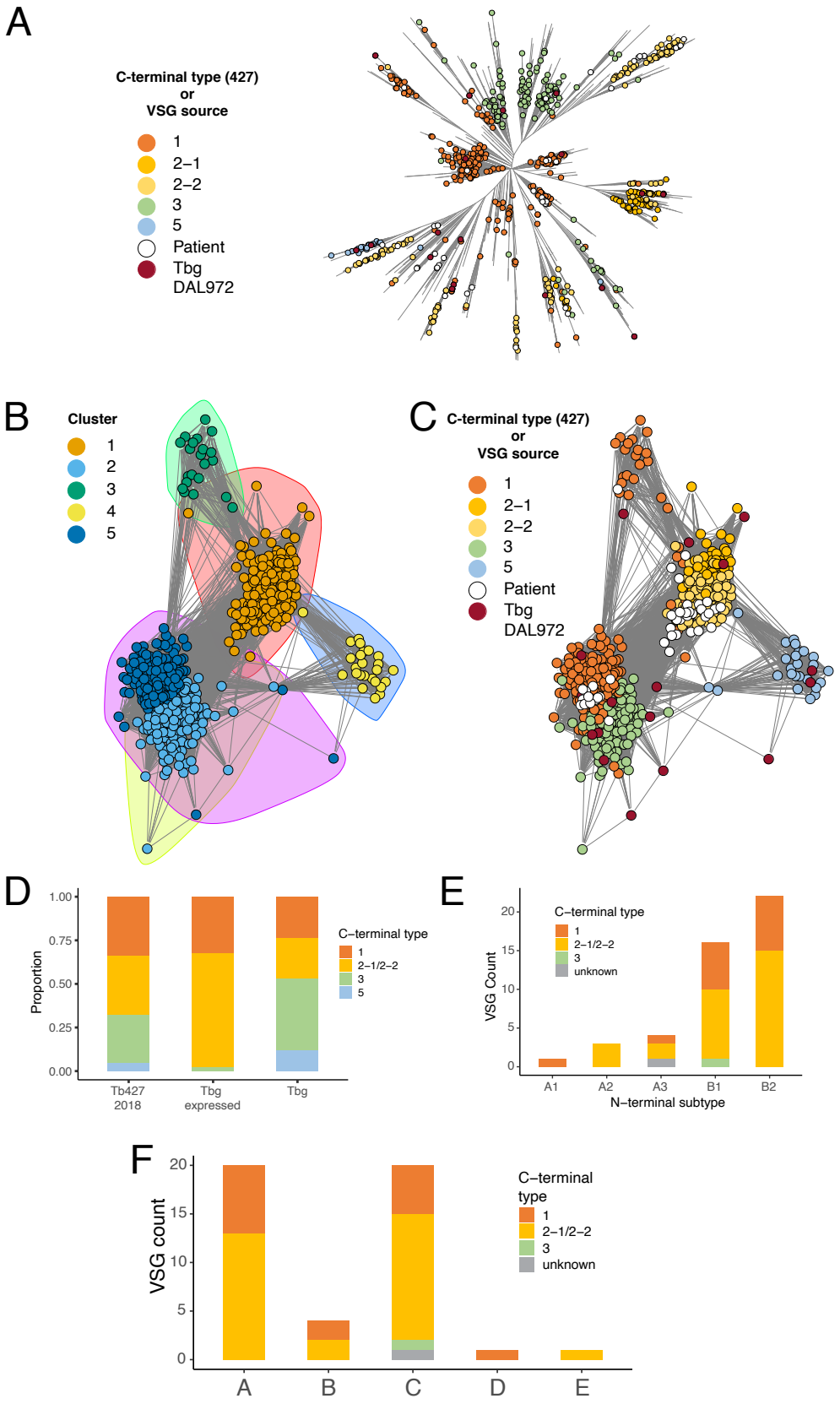
A
C-terminal type (427)
or
VSG source
1
2–1
2–2
3
5
Patient
Tbg
DAL972
B
Cluster
1
2
3
4
5
C
C-terminal type (427)
or
VSG source
1
2–1
2–2
3
5
Patient
Tbg
DAL972
D
Proportion
1.00
0.75
0.50
0.25
0.00
Tb427
2018
Tbg
expressed
Tbg
C–terminal type
1
2–1/2–2
3
5
E
VSG Count
20
15
10
5
0
A1
A2
A3
B1
B2
N–terminal subtype
C–terminal type
1
2–1/2–2
3
unknown
F
VSG count
20
15
10
5
0
A
B
C
D
E
C–terminal
type
1
2–1/2–2
3
unknown

606

607 **Figure 6. Expressed VSG C-termini are primarily type 1 and type 2.** A) BLASTp tree of C-
608 terminal domains. Points are colored based on previously-determined C-terminal type from
609 Cross et al., or by the source of the sequence (genomic or expressed) for *T. b. gambiense*
610 *VSGs*. B) Network plot showing peptide sequence relatedness between C-terminal domains in
611 *T. b. gambiense* expressed VSGs. Each point represents a VSG C-terminus; a link was drawn
612 between points if BLASTp e-value was less than $1x10^{-3}$. Points are colored by cluster
613 determined by the clustering algorithm. Clusters are also indicated by shaded circles. C) Same
614 network plot as in B, but colored by previously-determined C-terminal type from Cross et al., or
615 by source for unclassified genomic or expressed *VSGs*. D) VSG C-terminal types, based on
616 cluster assignment visualized in panel B, in genomic and expressed *VSG* sets. E) Pairing of C-
617 and N-termini in *T. b. gambiense* patients. F) C-termini detected in each patient village.

Discussion

African trypanosomes evade the host adaptive immune response through a process of antigenic variation, where parasites switch their expressed *VSG* [60]. The genome of *T. brucei* encodes a large repertoire of *VSG* genes, pseudogenes, and gene fragments, and can be extended continuously through recombination to form entirely novel "mosaic" *VSGs* [17]. While antigenic variation has been studied extensively in culture and in animal models of infection, our understanding of the process in natural infections, particularly human infection, is limited. Most experimental mouse infections are sustained for weeks to months, while humans and large mammals may be infected for several months or even years. Additionally, laboratory studies of antigenic variation almost exclusively use *T. b. brucei*, a subspecies of *T. brucei* that, by definition, does not infect humans.

The primary hurdle to exploring antigenic variation in nature has been technical; it is difficult to obtain sufficient parasite material for analysis. This is especially true for infection with *T. b. gambiense,* which often exhibits extremely low parasitemia. VSG-seq, which relies on PCR and requires very small amounts of material for analysis, provides a new tool for exploring *VSG* expression in natural human infections. Here we have demonstrated the feasibility of VSG-seq to analyze *VSG* expression in RNA samples isolated directly from HAT patients. Our analyses show that the diversity seen in mouse models of infection is mostly recapitulated in natural infection, but that there may be unique aspects of antigenic variation in *T. b. gambiense* that can only be explored by studying natural infections.

In our previous analysis of mouse infections, the most notable result was the diversity of *VSGs* expressed. Rather than a few *VSGs* expressed at a time, we saw many *VSGs* expressed simultaneously in the populations, confirming previous estimates of antigenic diversity in experimental mouse infection [17] and suggesting that the genomic *VSG* repertoire might be exploited very rapidly. In the study presented here, we detected several expressed *VSGs* in most *T. b. gambiense* samples. Although diversity in *T. b. gambiense* infection appeared lower overall, the correlation we observed between parasitemia and diversity in *T. b. gambiense* isolates specifically suggests that our sampling was incomplete. Indeed, in our analysis of *T. b. rhodesiense* infection (a more reasonable comparison to mouse infection given similar expression cutoffs and parasitemia), we observed diversity similar to or higher than what we have detected in *T. b. brucei* mouse infections. Moreover, *T. b. rhodesiense* patient CSF revealed another layer of diversity in *VSG* expression, with 5 *VSGs* expressed exclusively in this space. Overall, our analysis of *VSG* expression in *T. b. gambiense* and *T. b. rhodesiense* patients confirmed the long-held assumption that *VSG* diversity is a feature of natural infection.

While analyzing the sets of expressed *VSGs* in *T. b. gambiense* and *T. b. rhodesiense* infections, we found evidence for another feature of experimental infection that holds true in a natural host: hierarchical *VSG* expression. Both *in vitro* and *in vivo* studies have shown that *VSG* switching is not entirely stochastic but rather hierarchical, with

664 certain variants dominating expression in the parasite population in a reproducible order
665 that appears to be independent of the starting *VSG* [17,31,32,61,62]. Switching
666 hierarchy is hypothesized to be determined by multiple factors including homology,
667 gene size, and genomic location. In the *T. b. gambiense* samples, we found two *VSGs*
668 that met our detection threshold in multiple patients, and in *T. b. rhodesiense* a large
669 proportion of expressed *VSGs* were shared among multiple patients. Given the large
670 size of the genomic *VSG* repertoire, any overlap in expressed *VSG* repertoire is likely
671 indicative of a semi-predictable hierarchy of switching and preference for the expression
672 of certain *VSGs*.
673
674 Of the two shared *VSGs* we identified in the *T. b. gambiense* patients, one was
675 identified in two patients from the same village, while the other was found in two
676 patients from villages 40km apart. At this short distance, it is possible that the infecting
677 parasites were genetically similar and thus this overlap simply reflects preference in
678 switching. It would be interesting to investigate, however, whether preference for the
679 expression of certain *VSGs* occurs even between parasites isolated at greater
680 distances. Indeed, it has been shown that the sensitivity of serological tests for gHAT,
681 which detect antibody against the LiTat 1.3 VSG, vary regionally, potentially due to
682 differences in the underlying genomic or expressed *VSG* repertoire in circulating strains
683 [63,64]. Along these same lines, none of our assembled *T. b. gambiense VSGs* from
684 patients in the DRC shared significant similarity with those in the genome of DAL972, a
685 parasite isolate from Côte d'Ivoire. This could suggest that there are geographic
686 variations in *T. brucei VSG* repertoires. Similar variation has been observed in *var* gene
687 repertoires of *Plasmodium falciparum* [65] and the *VSG* repertoire of *Trypanosoma*
688 *vivax*, another African trypanosome [35]. A better understanding of such differences in
689 *T. brucei*, if they exist, could lead to development of more sensitive HAT diagnostics.
690
691 To better understand the VSG proteins expressed in natural infections, we developed
692 an HMM VSG typing pipeline that revealed an intriguing bias in *T. b. gambiense*
693 infection towards type B VSGs that appears to be specific to *T. b. gambiense* patient
694 samples. While small sample sizes and important differences between each *T. brucei*
695 subspecies' dataset limit the conclusions that can be drawn, comparisons between
696 these sets do suggest that the genomic *VSG* repertoire determines the distribution of
697 VSG N-terminal types expressed during *T. brucei* infection and may account for the bias
698 we have observed in *T. b. gambiense* patients.
699
700 Our analysis of experimental mouse infections suggests that while the predominant
701 expressed N-terminal domain type fluctuates between type A and type B over time,
702 even into advanced stages of infection, the repertoire expressed over the course of an
703 infection generally reflects the composition of the genomic *VSG* repertoire of the
704 infecting parasite strain. A direct comparison between the genomic *VSG* repertoire and
705 the expressed *VSG* repertoire can be made for experimental *T. b. brucei* EATRO1125
706 infections, as the EATRO1125 VSGnome was generated from the same parasite strain
707 used to initiate these infections. Such a direct comparison is impossible for patient
708 samples. While the content of the 'core' *T. brucei* genome (containing the diploid,
709 housekeeping genes) is similar enough among subspecies for resequencing projects to

710 be scaffolded using the TREU927 or Lister 427 reference genomes [59,66,67], it is not
711 clear whether the *VSG* repertoires of subspecies (or even individual parasite strains
712 [36]) share this degree of similarity. Although a near-complete VSGnome for any *T. b.*
713 *rhodesiense* strain was not available, we chose to compare the makeup of *T. b.*
714 *rhodesiense* expressed *VSGs* with the well-characterized genome of *T. b. brucei* Lister
715 427 [16], given the extreme similarity between *T. b. brucei* and *T. b. rhodesiense* [59].
716 Similarly, we compared expressed *VSGs* in *T. b. gambiense* patients to the limited set
717 of *VSGs* in the *T. b. gambiense* DAL972 genome. In both cases, the distribution of N-
718 terminal types expressed in infection was not significantly different from that of the
719 genomic *VSG* repertoire to which the expressed *VSGs* were being compared. Taken
720 together, these data support a model in which VSG types are drawn from the repertoire
721 at roughly equal frequency to their representation in the genome, and that that the *T. b.*
722 *gambiense VSG* repertoire may contain a larger proportion of type B VSG than its more
723 virulent counterparts.
724
725 Another possibility we cannot rule out is that the gHAT samples are biased due to
726 selection by the serological test used for diagnosis. Patients were screened for *T. b.*
727 *gambiense* infection using the CATT, a serological test that uses parasites expressing
728 VSG LiTat 1.3 as an antigen. LiTat 1.3 contains a type B2 N-terminal domain [63,64]. It
729 is possible that patients infected with parasites predominantly expressing type B VSGs
730 are more likely to generate antibodies that cross-react with LiTat1.3, resulting in
731 preferential detection of these cases. In contrast, *T.b. rhodesiense* can only be
732 diagnosed microscopically, removing the potential to introduce bias through screening.
733 It remains to be investigated whether samples from patients diagnosed using newer
734 screening tests, which include the invariant surface glycoprotein ISG65 and the type A
735 VSG LiTat 1.5 [29], would show similar bias towards expression of type B VSGs.
736
737 Analysis of expressed VSG C-terminal domains in *T. b. gambiense* patients showed a
738 bias towards C-terminal types 1 and 2. The diagnostic VSG LiTat1.3 contains a type 3
739 C-terminus, a C-terminal type which was underrepresented in the patient set. Therefore,
740 it is unlikely that a bias in expressed C-terminal types is related to the screening
741 method. Notably, the bias towards C-terminal types 1 and 2 was not reflected in the
742 limited *VSG* repertoire of the DAL972 reference genome or the repertoire of the Lister
743 427 *T. b. brucei* reference genome. This could be related to the limited set of *VSG*s
744 present in the DAL972 reference genome, or it could suggest a true bias in expression.
745
746 Could a bias towards certain VSG types, whether due to a difference in repertoire
747 composition or expression preference, account for the chronic nature of gHAT? While
748 the genomic *VSG* repertoire has been analyzed extensively in laboratory strains, little is
749 known about how differences in VSG proteins relate to parasite biology or whether there
750 could be biological consequences to the expression of specific VSG N- or C-terminal
751 types. Type A *var* genes in *Plasmodium falciparum* infection have been shown to be
752 associated with severe malaria [68–72], and similar mechanisms have been
753 hypothesized to exist in *T. vivax* and *T. congolense* infections [33,35,73,74]. In *T.*
754 *brucei,* several VSGs have evolved specific functions besides antigenic variation [74].
755 Recently, the first type B VSG structure was solved [75], revealing a unique *O*-linked

carbohydrate in the VSG's N-terminal domain. This modification was found to interfere with the generation of protective immunity in a mouse model of infection; perhaps structural differences between each VSG type, including patterns of glycosylation, could influence infection outcomes. Further research will be needed to determine whether the observed predominance of type B VSGs could influence the clinical presentation of *T. b. gambiense* infection.

Currently, it is unclear why this collection of gHAT patient isolates demonstrates a bias towards expression of certain VSG types. More research will be needed to determine whether the *T. b. gambiense VSG* repertoire contains a unique distribution of VSG types, whether these parasites preferentially express certain VSG types, and whether this bias could have functional consequences. What this study has shown, however, is that it is feasible to explore antigenic variation in natural infection and that, although mouse models do reflect the general dynamics of antigenic variation in natural *T. brucei* infection, unique biology remains to be uncovered by studying antigenic variation in its natural context.

Acknowledgments

We are very grateful to the patients without whom this work would not have been possible. We thank George Cross and Danae Schulz for comments on the manuscript. We would also like to thank Mary Gebhardt for help with GIS. The atlas of HAT is an initiative of the World Health Organization (WHO), jointly implemented with the Food and Agriculture Organization of the United Nations (FAO) in the framework of the Programme Against African Trypanosomosis (PAAT).

785 # Supplement

786

787 **Supplemental Table 1. Primer sequences.**

788

789 **Supplemental Table 2. gHAT patient distance matrix.**

790

791 **Supplemental Table 3. gHAT VSG expression data.**

792

793 **Supplemental Table 4. Tables comparing BLAST-tree, HMMscan, and network plot typing**
794 **methods.**

795

796 **Supplemental Table 5. rHAT VSG expression data.**

797

798

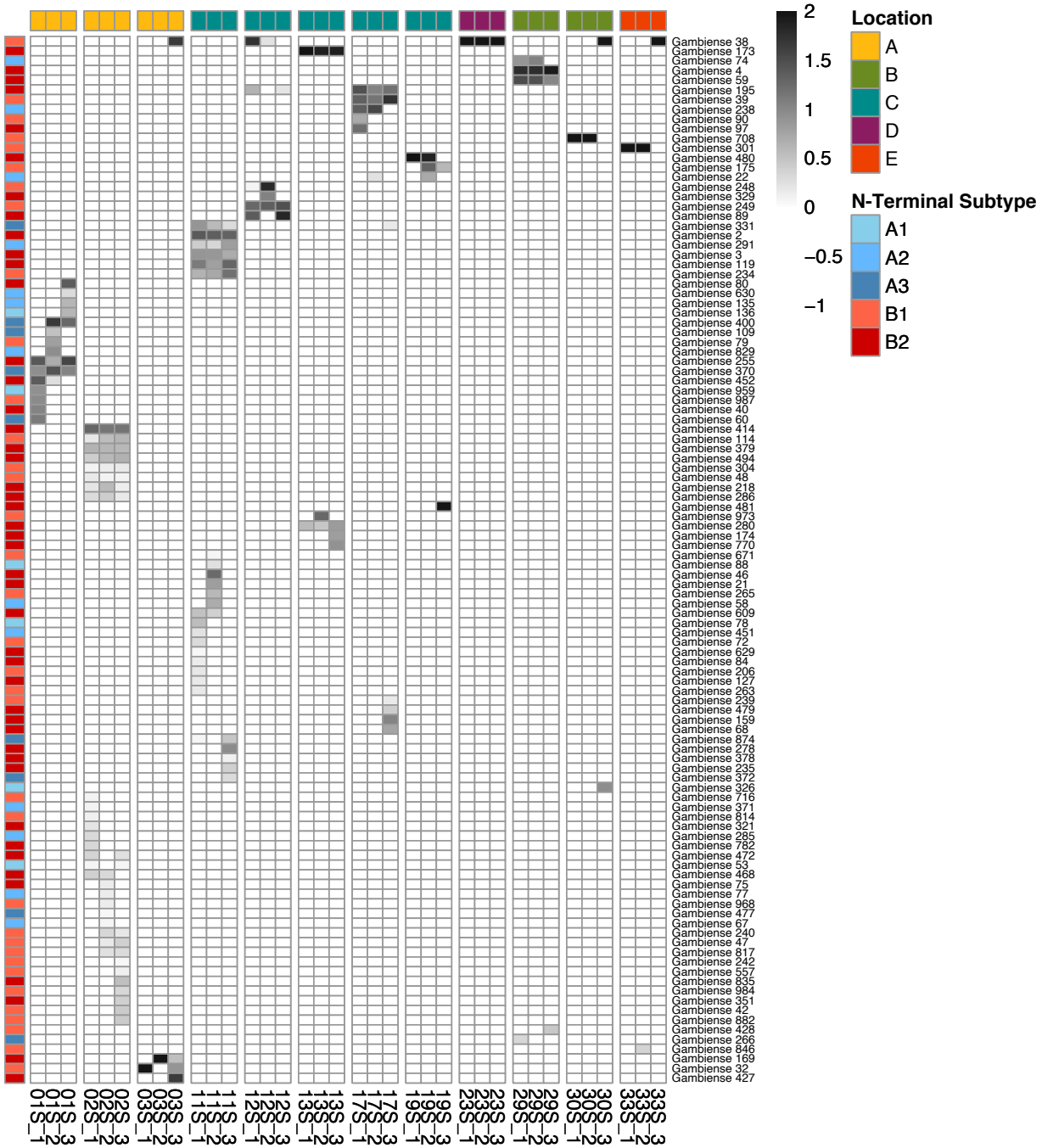

Supplemental Figure 1. Heatmap of all assembled *T.b. gambiense* patient VSGs

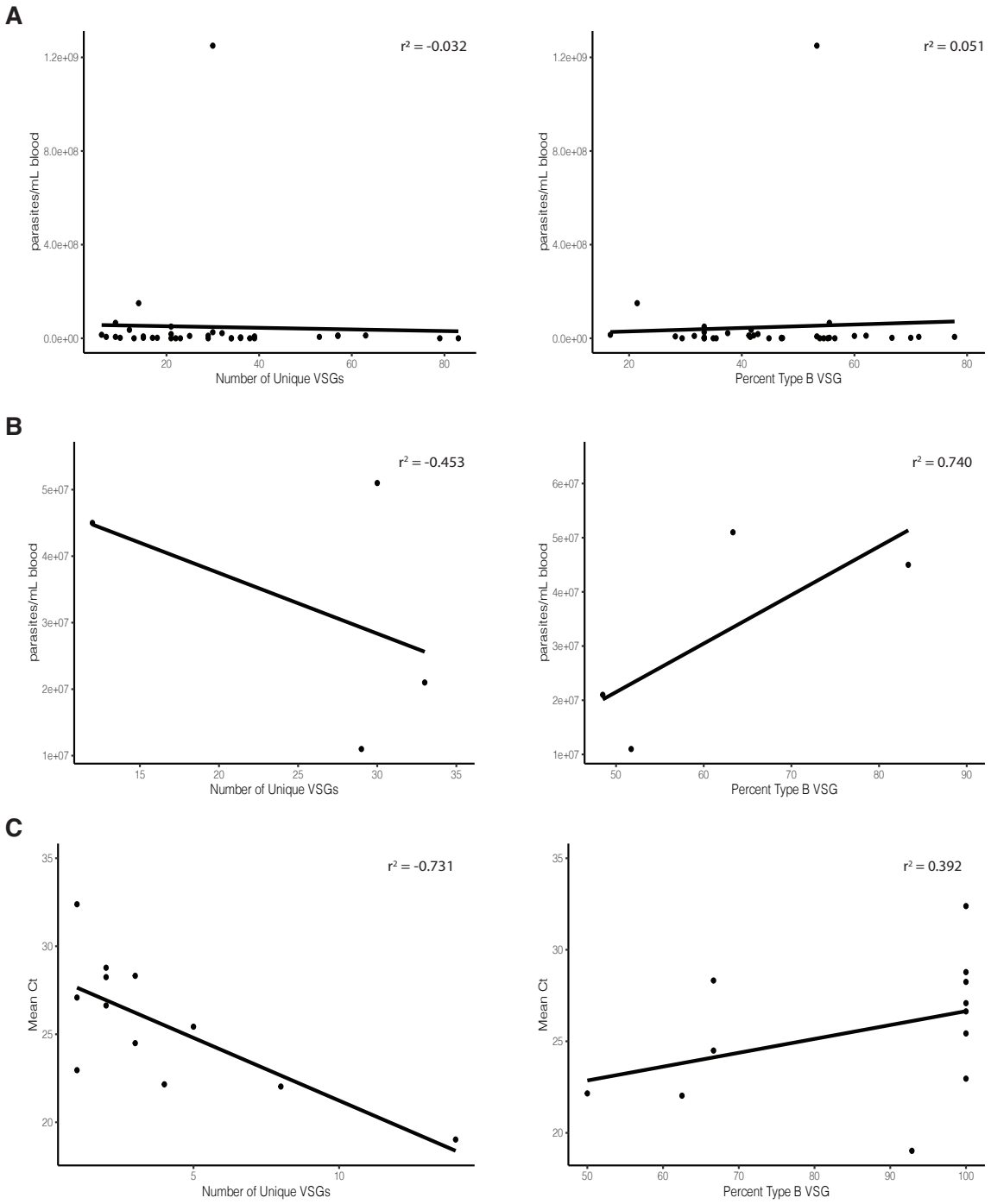

Supplemental Figure 2. Correlation between parasitemia and diversity and N-terminal type distribution. (A) Correlation plots for VSG diversity and percent of N-terminal domain type B for *T.b. brucei* infected mice from Mugnier et.al 2015. (B) Correlation plots for *T.b. rhodesiense* infected patients from Mulindwa et. al. 2018. (C) Correlation plots for *T.b. gambiense* infected patients.

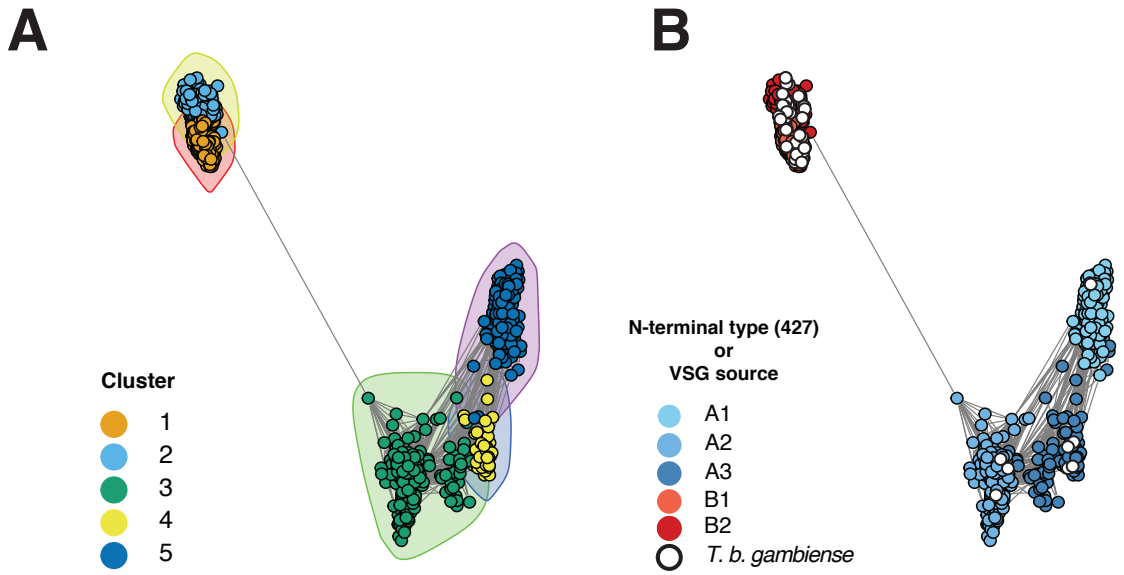

Supplemental Figure 3. (A) Network plot showing peptide sequence relatedness between N-terminal domains. Each point represents a VSG N-terminus. A link was drawn between points if BLASTp e-value was less than 10^{-2}. Colors and shaded circles represent community assignment determined by the clustering algorithm. (B) Same graph as in (A), but points are manually colored by known N-terminal subtype from Cross et al., or by subspecies for VSGs identified in patients.

820
821 **Supplemental Fig 4. BLASTp-tree of all *T. b. gambiense VSGs.*** File attached.
822

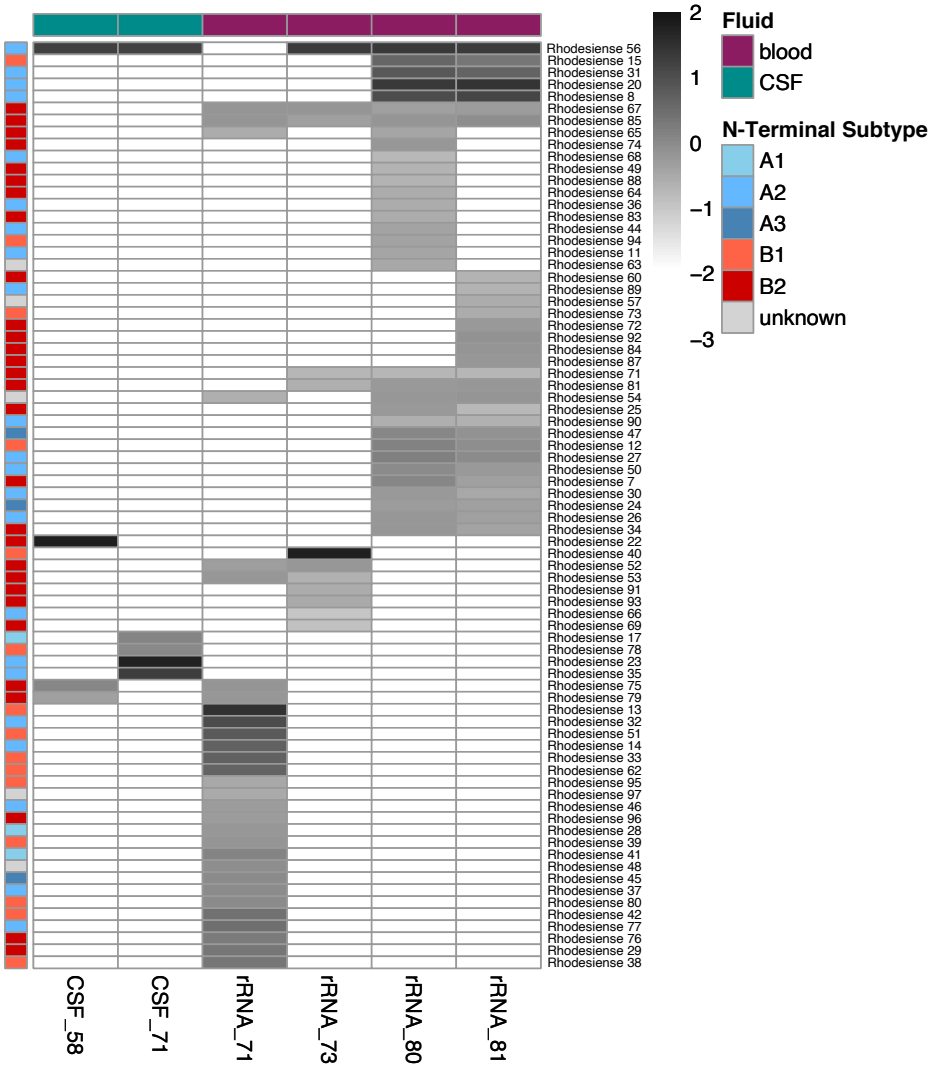

Supplemental Figure 5. Heatmap of all assembled *T.b. rhodesiense* patient VSGs

References

1. Romero-Meza G, Mugnier MR. Trypanosoma brucei. Trends in Parasitology. 2019. doi:10.1016/j.pt.2019.10.007
2. Büscher P, Cecchi G, Jamonneau V, Priotto G. Human African trypanosomiasis. www.thelancet.com. 2017;390. doi:10.1016/S0140-6736(17)31510-6
3. Franco JR, Cecchi G, Priotto G, Paone M, Diarra A, Grout L, et al. Monitoring the elimination of human African trypanosomiasis at continental and country level: Update to 2018. PLoS Negl Trop Dis. 2020;14: e0008261. doi:10.1371/JOURNAL.PNTD.0008261
4. Kennedy PGE, Rodgers J. Clinical and neuropathogenetic aspects of human African trypanosomiasis. Frontiers in Immunology. Frontiers Media S.A.; 2019. doi:10.3389/fimmu.2019.00039
5. Franco JR, Cecchi G, Priotto G, Paone M, Diarra A, Grout L, et al. Monitoring the elimination of human African trypanosomiasis at continental and country level: Update to 2018. PLoS Negl Trop Dis. 2020;14: e0008261. doi:10.1371/JOURNAL.PNTD.0008261
6. WHO. The Global Health Observatory. In: WHO [Internet]. World Health Organization; [cited 17 Aug 2021]. Available: https://www.who.int/data/gho/data/themes/topics/indicator-groups/indicator-group-details/GHO/human-african-trypanosomiasis
7. WHO. Ending the neglect to attain the sustainable development goals: a road map for neglected tropical diseases 2021–2030. Geneva; 2020.
8. Magez S, Caljon G, Tran T, Stijlemans B, Radwanska M. Current status of vaccination against African trypanosomiasis. Parasitology. 2010;137: 2017–2027.
9. Trindade S, Rijo-Ferreira F, Carvalho T, Pinto-Neves D, Guegan F, Aresta-Branco F, et al. Trypanosoma brucei Parasites Occupy and Functionally Adapt to the Adipose Tissue in Mice. Cell Host Microbe. 2016;19: 837–848. doi:10.1016/j.chom.2016.05.002
10. Pereira SS, Trindade S, De Niz M, Figueiredo LM. Tissue tropism in parasitic diseases. Open Biology. Royal Society Publishing; 2019. doi:10.1098/rsob.190036
11. Camara M, Soumah AM, Ilboudo H, Travaillé C, Clucas C, Cooper A, et al. Extravascular Dermal Trypanosomes in Suspected and Confirmed Cases of gambiense Human African Trypanosomiasis. Clin Infect Dis. 2021;73: 12–20. doi:10.1093/cid/ciaa897
12. Alfituri OA, Bradford BM, Paxton E, Morrison LJ, Mabbott NA. Influence of the Draining Lymph Nodes and Organized Lymphoid Tissue Microarchitecture on Susceptibility to Intradermal Trypanosoma brucei Infection. Front Immunol. 2020;11. doi:10.3389/fimmu.2020.01118
13. Marcello L, Barry JD. Analysis of the VSG gene silent archive in Trypanosoma brucei reveals that mosaic gene expression is prominent in antigenic variation and is favored by archive substructure. Genome Res. 2007;17: 1344–1352.
14. Berriman M, Ghedin E, Hertz-Fowler C, Blandin G, Renauld H, Bartholomeu DC, et al. The genome of the African trypanosome Trypanosoma brucei. Sci (New York, NY). 2005;309: 416–422.
15. Cross GAM, Kim H-S, Wickstead B. Capturing the variant surface glycoprotein

repertoire (the VSGnome) of Trypanosoma brucei Lister 427. Mol Biochem Parasitol. 2014;195: 59–73. doi:10.1016/j.molbiopara.2014.06.004

16. Müller LSM, Cosentino RO, Förstner KU, Guizetti J, Wedel C, Kaplan N, et al. Genome organization and DNA accessibility control antigenic variation in trypanosomes. Nature. 2018;563: 121–125.
17. Hall JPJ, Wang H, Barry JD. Mosaic VSGs and the scale of Trypanosoma brucei antigenic variation. Horn D, editor. PLoS Pathog. 2013;9: e1003502.
18. Jayaraman S, Harris C, Paxton E, Donachie A-M, Vaikkinen H, McCulloch R, et al. Application of long read sequencing to determine expressed antigen diversity in Trypanosoma brucei infections. Acosta-Serrano A, editor. PLoS Negl Trop Dis. 2019;13: e0007262. doi:10.1371/journal.pntd.0007262
19. Carrington M, Miller N, Blum M, Roditi I, Wiley D, Turner M. Variant specific glycoprotein of Trypanosoma brucei consists of two domains each having an independently conserved pattern of cysteine residues. J Mol Biol. 1991;221: 823–835.
20. Hutchinson OC, Smith W, Jones NG, Chattopadhyay A, Welburn SC, Carrington M. VSG structure: similar N-terminal domains can form functional VSGs with different types of C-terminal domain. Mol Biochem Parasitol. 2003;130: 127–131.
21. Jones NG, Nietlispach D, Sharma R, Burke DF, Eyres I, Mues M, et al. Structure of a glycosylphosphatidylinositol-anchored domain from a trypanosome variant surface glycoprotein. J Biol Chem. 2008;283: 3584–3593.
22. Schwede A, Jones N, Engstler M, Carrington M. The VSG C-terminal domain is inaccessible to antibodies on live trypanosomes. Mol Biochem Parasitol. 2011;175: 201–204.
23. Van Meirvenne N, Magnus E, Büscher P. Evaluation of variant specific trypanolysis tests for serodiagnosis of human infections with Trypanosoma brucei gambiense. Acta Trop. 1995;60: 189–199. doi:10.1016/0001-706X(95)00127-Z
24. A card-agglutination test with stained trypanosomes (C. A. T.T.) for the serological diagnosis of T. b. gambiense tripanosomiasis. [cited 8 Sep 2021]. Available: https://www.cabdirect.org/cabdirect/abstract/19792901755
25. Dukes P, Gibson WC, Gashumba JK, Hudson KM, Bromidge TJ, Kaukus A, et al. Absence of the LiTat 1.3 (CATT antigen) gene in Trypanosoma brucei gambiense stocks from Cameroon. Acta Trop. 1992.
26. Enyaru JCK, Allingham R, Bromidge T, Kanmogne GD, Carasco JF. The isolation and genetic heterogeneity of Trypanosoma brucei gambiense from north-west Uganda. Acta Trop. 1993.
27. Bisser S, Lumbala C, Nguertoum E, Kande V, Flevaud L, Vatunga G, et al. Sensitivity and Specificity of a Prototype Rapid Diagnostic Test for the Detection of Trypanosoma brucei gambiense Infection: A Multi-centric Prospective Study. Acosta-Serrano A, editor. PLoS Negl Trop Dis. 2016;10: e0004608. doi:10.1371/journal.pntd.0004608
28. Büscher P, Mertens P, Leclipteux T, Gilleman Q, Jacquet D, Mumba-Ngoyi D, et al. Sensitivity and specificity of HAT Sero-K-SeT, a rapid diagnostic test for serodiagnosis of sleeping sickness caused by Trypanosoma brucei gambiense: A case-control study. Lancet Glob Heal. 2014;2: e359–e363. doi:10.1016/S2214-109X(14)70203-7

29. Lumbala C, Biéler S, Kayembe S, Makabuza J, Ongarello S, Ndung'u JM. Prospective evaluation of a rapid diagnostic test for Trypanosoma brucei gambiense infection developed using recombinant antigens. PLoS Negl Trop Dis. 2018;12: e0006386. doi:10.1371/JOURNAL.PNTD.0006386
30. Mugnier MR, Cross GAM, Papavasiliou FN. The in vivo dynamics of antigenic variation in Trypanosoma brucei. Science (80-). 2015;347: 1470–1473. doi:10.1126/science.aaa4502
31. Morrison LJ, Majiwa P, Read AF, Barry JD. Probabilistic order in antigenic variation of Trypanosoma brucei. Int J Parasitol. 2005;35: 961–972.
32. Lythgoe KA, Morrison LJ, Read AF, Barry JD. Parasite-intrinsic factors can explain ordered progression of trypanosome antigenic variation. Proc Natl Acad Sci U S A. 2007;104: 8095–8100.
33. Silva Pereira S, Heap J, Jones AR, Jackson AP. VAPPER: High-throughput variant antigen profiling in African trypanosomes of livestock. Gigascience. 2019;8. doi:10.1093/gigascience/giz091
34. Pereira SS, Casas-Sánchez A, Haines LR, Ogugo M, Absolomon K, Sanders M, et al. Variant antigen repertoires in Trypanosoma congolense populations and experimental infections can be profiled from deep sequence data using universal protein motifs. Genome Res. 2018;28: 1383–1394. doi:10.1101/gr.234146.118
35. Silva Pereira S, de Almeida Castilho Neto KJG, Duffy CW, Richards P, Noyes H, Ogugo M, et al. Variant antigen diversity in Trypanosoma vivax is not driven by recombination. Nat Commun. 2020;11: 844. doi:10.1038/s41467-020-14575-8
36. Hutchinson OC, Picozzi K, Jones NG, Mott H, Sharma R, Welburn SC, et al. Variant Surface Glycoprotein gene repertoires in Trypanosoma brucei have diverged to become strain-specific. BMC Genomics. 2007;8: 234. doi:10.1186/1471-2164-8-234
37. Ilboudo H, Noyes H, Mulindwa J, Kimuda MP, Koffi M, Kaboré JW, et al. Introducing the TrypanoGEN biobank: A valuable resource for the elimination of human African trypanosomiasis. PLoS Negl Trop Dis. 2017;11: e0005438. doi:10.1371/JOURNAL.PNTD.0005438
38. Camara M, Camara O, Ilboudo H, Sakande H, Kaboré J, N'Dri L, et al. Sleeping sickness diagnosis: use of buffy coats improves the sensitivity of the mini anion exchange centrifugation test. Trop Med Int Heal. 2010;15: 796–799. doi:10.1111/J.1365-3156.2010.02546.X
39. Simarro PP, Cecchi G, Paone M, Franco JR, Diarra A, Ruiz JA, et al. The Atlas of human African trypanosomiasis: A contribution to global mapping of neglected tropical diseases. Int J Health Geogr. 2010;9: 57. doi:10.1186/1476-072X-9-57
40. González-Andrade P, Camara M, Ilboudo H, Bucheton B, Jamonneau V, Deborggraeve S. Diagnosis of trypanosomatid infections: Targeting the spliced leader RNA. J Mol Diagnostics. 2014. doi:10.1016/j.jmoldx.2014.02.006
41. Brakenhoff RH, Schoenmakers JG, Lubsen NH. Chimeric cDNA clones: a novel PCR artifact. Nucleic Acids Res. 1991;19: 1949. doi:10.1093/NAR/19.8.1949
42. Meyerhans A, Vartanian J-P, Wain-Hobson S. DNA recombination during PCR. Nucleic Acids Res. 1990;18: 1687–1691. doi:10.1093/NAR/18.7.1687
43. Grabherr MG, Haas BJ, Yassour M, Levin JZ, Thompson DA, Amit I, et al. Full-length transcriptome assembly from RNA-Seq data without a reference genome.

968 Nat Biotechnol. 2011;29: 644–652.
969 44. Li W, Godzik A. Cd-hit: a fast program for clustering and comparing large sets of
970 protein or nucleotide sequences. Bioinformatics. 2006;22: 1658–1659.
971 45. Langmead B, Trapnell C, Pop M, Salzberg SL. Ultrafast and memory-efficient
972 alignment of short DNA sequences to the human genome. Genome Biol. 2009;10:
973 R25.
974 46. Storvall H, Ramsköld D, Sandberg R. Efficient and comprehensive representation
975 of uniqueness for next-generation sequencing by minimum unique length
976 analyses. PLoS One. 2013;8: e53822.
977 47. Wickstead B, Gull K. Dyneins across eukaryotes: a comparative genomic
978 analysis. Traffic. 2007;8: 1708–1721.
979 48. Howe K, Bateman A, Durbin R. QuickTree: Building huge neighbour-joining trees
980 of protein sequences. Bioinformatics. 2002;18: 1546–1547.
981 doi:10.1093/bioinformatics/18.11.1546
982 49. Paradis E, Schliep K. Ape 5.0: An environment for modern phylogenetics and
983 evolutionary analyses in R. Bioinformatics. 2019;35: 526–528.
984 doi:10.1093/bioinformatics/bty633
985 50. Sievers F, Wilm A, Dineen D, Gibson TJ, Karplus K, Li W, et al. Fast, scalable
986 generation of high-quality protein multiple sequence alignments using Clustal
987 Omega. Mol Syst Biol. 2011;7: 539–539. doi:10.1038/msb.2011.75
988 51. Eddy SR. Accelerated Profile HMM Searches. PLOS Comput Biol. 2011;7:
989 e1002195. doi:10.1371/JOURNAL.PCBI.1002195
990 52. Csárdi G, Nepusz T. The igraph software package for complex network research.
991 53. Newman MEJ. Finding community structure in networks using the eigenvectors of
992 matrices. Phys Rev E. 2006;74: 036104. doi:10.1103/PhysRevE.74.036104
993 54. González-Andrade P, Camara M, Ilboudo H, Bucheton B, Jamonneau V,
994 Deborggraeve S. Diagnosis of trypanosomatid infections: targeting the spliced
995 leader RNA. J Mol Diagn. 2014;16: 400–404.
996 55. Berberof M, Pérez-Morga D, Pays E. A receptor-like flagellar pocket glycoprotein
997 specific to Trypanosoma brucei gambiense. Mol Biochem Parasitol. 2001;113:
998 127–138.
999 56. Weirather JL, Wilson ME, Donelson JE. Mapping of VSG similarities in
1000 Trypanosoma brucei. Mol Biochem Parasitol. 2012;181: 141–152.
1001 57. Mulindwa J, Leiss K, Ibberson D, Kamanyi Marucha K, Helbig C, Melo do
1002 Nascimento L, et al. Transcriptomes of Trypanosoma brucei rhodesiense from
1003 sleeping sickness patients, rodents and culture: Effects of strain, growth
1004 conditions and RNA preparation methods. Salavati R, editor. PLoS Negl Trop Dis.
1005 2018;12: e0006280.
1006 58. De Greef C, Hamers R. The serum resistance-associated (SRA) gene of
1007 Trypanosoma brucei rhodesiense encodes a variant surface glycoprotein-like
1008 protein. Mol Biochem Parasitol. 1994;68: 277–284.
1009 59. Sistrom M, Evans B, Benoit J, Balmer O, Aksoy S, Caccone A. De Novo Genome
1010 Assembly Shows Genome Wide Similarity between Trypanosoma brucei brucei
1011 and Trypanosoma brucei rhodesiense. Louis EJ, editor. PLoS One. 2016;11:
1012 e0147660. doi:10.1371/journal.pone.0147660
1013 60. Mugnier MR, Stebbins CE, Papavasiliou FN. Masters of Disguise: Antigenic

Variation and the VSG Coat in Trypanosoma brucei. Knoll LJ, editor. PLOS Pathog. 2016;12: e1005784. doi:10.1371/journal.ppat.1005784

61. Aitcheson N, Talbot S, Shapiro J, Hughes K, Adkin C, Butt T, et al. VSG switching in Trypanosoma brucei: antigenic variation analysed using RNAi in the absence of immune selection. Mol Microbiol. 2006;57: 1608–1622. doi:10.1111/j.1365-2958.2005.04795.x.VSG

62. Liu D, Albergante L, Newman TJ, Horn D. Faster growth with shorter antigens can explain a VSG hierarchy during African trypanosome infections: a feint attack by parasites. Sci Rep. 2018;8: 10922. doi:10.1038/s41598-018-29296-8

63. Chappuis F, Loutan L, Simarro P, Lejon V, Büscher P. Options for field diagnosis of human african trypanosomiasis. Clin Microbiol Rev. 2005;18: 133–146.

64. Truc P, Lejon V, Magnus E, Jamonneau V, Nangouma A, Verloo D, et al. Evaluation of the micro-CATT, CATT/Trypanosoma brucei gambiense, and LATEX/T b gambiense methods for serodiagnosis and surveillance of human African trypanosomiasis in West and Central Africa. Bull World Health Organ. 2002;80: 882–886.

65. Tonkin-Hill G, Ruybal-Pesántez S, Tiedje KE, Rougeron V, Duffy MF, Zakeri S, et al. Evolutionary analyses of the major variant surface antigen-encoding genes reveal population structure of Plasmodium falciparum within and between continents. PLOS Genet. 2021;17: e1009269. doi:10.1371/JOURNAL.PGEN.1009269

66. Jackson AP, Sanders M, Berry A, McQuillan J, Aslett MA, Quail MA, et al. The genome sequence of Trypanosoma brucei gambiense, causative agent of chronic human African Trypanosomiasis. PLoS Negl Trop Dis. 2010;4. doi:10.1371/journal.pntd.0000658

67. Sistrom M, Evans B, Bjornson R, Gibson W, Balmer O, Maser P, et al. Comparative genomics reveals multiple genetic backgrounds of human pathogenicity in the trypanosoma brucei complex. Genome Biol Evol. 2014;6: 2811–2819. doi:10.1093/gbe/evu222

68. Kirchgatter K, del Portillo HA. Association of Severe Noncerebral Plasmodium falciparum Malaria in Brazil With Expressed PfEMP1 DBL1α Sequences Lacking Cysteine Residues. Mol Med 2002 81. 2002;8: 16–23. doi:10.1007/BF03401999

69. Bull PC, Berriman M, Kyes S, Quail MA, Hall N, Kortok MM, et al. Plasmodium falciparum Variant Surface Antigen Expression Patterns during Malaria. PLOS Pathog. 2005;1: e26. doi:10.1371/JOURNAL.PPAT.0010026

70. Abdi AI, Hodgson SH, Muthui MK, Kivisi CA, Kamuyu G, Kimani D, et al. Plasmodium falciparum malaria parasite var gene expression is modified by host antibodies: longitudinal evidence from controlled infections of Kenyan adults with varying natural exposure. BMC Infect Dis 2017 171. 2017;17: 1–11. doi:10.1186/S12879-017-2686-0

71. Kyriacou HM, Stone GN, Challis RJ, Raza A, Lyke KE, Thera MA, et al. Differential var gene transcription in Plasmodium falciparum isolates from patients with cerebral malaria compared to hyperparasitaemia. Mol Biochem Parasitol. 2006;150: 211–218. doi:10.1016/J.MOLBIOPARA.2006.08.005

72. Duffy F, Bernabeu M, Babar PH, Kessler A, Wang CW, Vaz M, et al. Meta-analysis of plasmodium falciparum var signatures contributing to severe Malaria in

African children and Indian adults. MBio. 2019;10. doi:10.1128/MBIO.00217-19

73. Pereira SS, Casas-Sánchez A, Haines LR, Ogugo M, Absolomon K, Sanders M, et al. Variant antigen repertoires in Trypanosoma congolense populations and experimental infections can be profiled from deep sequence data using universal protein motifs. Genome Res. 2018;28: 1383. doi:10.1101/GR.234146.118

74. Silva Pereira S, Jackson AP, Figueiredo LM. Evolution of the variant surface glycoprotein family in African trypanosomes. Trends Parasitol. 2021. doi:10.1016/J.PT.2021.07.012

75. Pinger J, Nešić D, Ali L, Aresta-Branco F, Lilic M, Chowdhury S, et al. African trypanosomes evade immune clearance by O-glycosylation of the VSG surface coat. Nat Microbiol. 2018;19: 53.